AD-A073 552   WASHINGTON UNIV ST LOUIS MO SEMICONDUCTOR RESEARCH LAB   F/G 14/2
                GAAS WAVEGUIDE DETECTOR ARRAY FOR AN IOC SPECTRUM ANALYZER.(U)
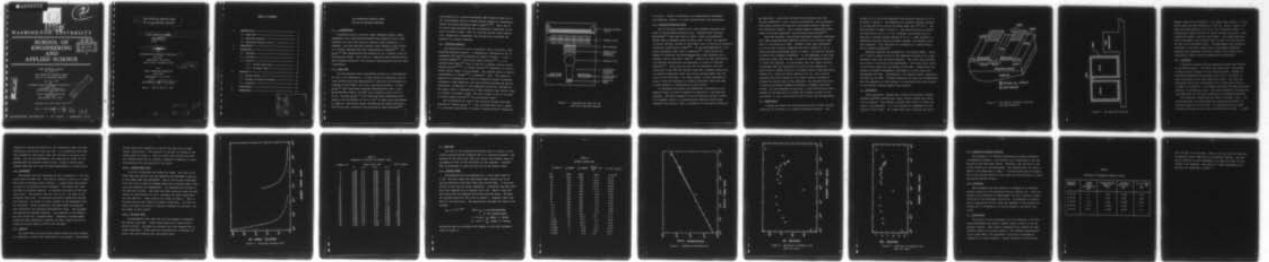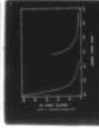   JUL 79   N00173-78-C-0134
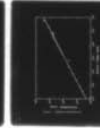UNCLASSIFIED   64351-1   NL

1 OF 1
AD
A073552

END
DATE
FILMED
10-79
DDC

MICROCOPY RESOLUTION TEST CHART

NATIONAL BUREAU OF STANDARDS-1963-A

LEVEL II

WASHINGTON UNIVERSITY

SCHOOL OF ENGINEERING AND APPLIED SCIENCE

FINAL TECHNICAL REPORT
No. 64351-1

GaAs WAVEGUIDE DETECTOR ARRAY

FOR AN IOC SPECTRUM ANALYZER

July 31, 1979
By
Semiconductor Research Laboratory
Box 1127
Washington University
Saint Louis, Missouri 63130
For
Naval Research Laboratory
Code 5262
Washington, D.C. 20375

Contract No. N00173-78-C-0134

June 1, 1978 to May 31, 1979

79 08 06 033

WASHINGTON UNIVERSITY / ST. LOUIS / MISSOURI 63130

GaAs WAVEGUIDE DETECTOR ARRAY

FOR AN IOC SPECTRUM ANALYZER

FINAL TECHNICAL REPORT. 1 Jun 78-31 May 79.

NO. 64351-1

31 July 1979

By

Semiconductor Research Laboratory

Box 1127

Washington University

Saint Louis, Missouri 63130

For

Naval Research Laboratory

Code 5262

Washington, D.C. 20375

Contract No. N00173-78-C-0134

June 1, 1978 to May 31, 1979

411361

79 08 06 033

TABLE OF CONTENTS

GaAs WAVEGUIDE DETECTOR ARRAY
FOR AN IOC SPECTRUM ANALYZER

1.   INTRODUCTION

Integrated optical circuits (IOCs) combining optical signal propagation with high-speed photoelectronic detection have a high potential for very fast analog or digital signal processing. A wideband, real-time spectrum analyzer using thermally grown oxides on a silicon substrate has been investigated by Anderson[1]. Sun et al.[2] have demonstrated the feasibility of a 3-channel time de-multiplexing scheme. Data rates of 1 Mbps have been achieved using GaAs waveguide detectors, and frequency demultiplexing has also been investigated.

1.1   GaAs IOCs

Gallium Arsenide shows considerable promise as a semiconductor for use in IOC fabrication. A large variety of electronic and optical devices have been demonstrated in GaAs with the desirable attributes of high speed, low noise, and high efficiency. Lindley et al.[3] have fabricated avalanche photodetectors with a large gain-bandwidth product (<50 GHz) and a signal-to-noise ratio of 30 dB. Stillman et al.[4] have fabricated GaAs waveguides which operate with attenuation as low as 2 cm^{-1} at GaAs laser wavelengths. In addition, GaAs-AlGaAs double heterostructure lasers emitting at 9100 Å have been integrated with high-purity GaAs waveguides[5].

Electroabsorption avalanch photodiode (EAP) detectors make use of
the Franz-Keldysh effect to detect optical signals at frequencies
beyond the normal absorption edge of GaAs[2,6-8]. Their use as
an output stage provides the key to monolithic integration of op-
tical circuits in GaAs: that is, with EAP devices signal genera-
tion, propagation, processing, and optoelectronic decoding are
possible on a single substrate.

1.2   Spectrum Analysis

One application for such a monolithic IOC is real-time, wide-
bandwidth spectrum analysis. A hypothetical configuration for an
integrated GaAs spectrum analyzer is shown in Figure 1. A dis-
tributed feedback[9], distributed Bragg reflector[10], or in-
tegrated Fabry-Perot[5] laser is used as a coherent optical source.
Acousto-optical[11,12] or electro-optical[13] deflection is used to
encode the RF signal to be processed. The encoded signal is Fourier
transformed by a Fresnel[14] or Luneburg[1] lens. The resulting
spectrum is collected by an array of integrated channel waveguides
terminated in EAP detectors, and these detectors decode the optical
information, converting it into compatible electrical information.
The signal level is regulated by on-chip automatic gain control (AGC)
to increase the dynamic range. The final signal is fed to an array
of charge coupled devices[15] for multiplexed output.

The requirements for such an IOC spectrum analyzer have been
examined by Anderson et al.[1]. They concluded that such a system
is a realizable application of present integrated optics technology
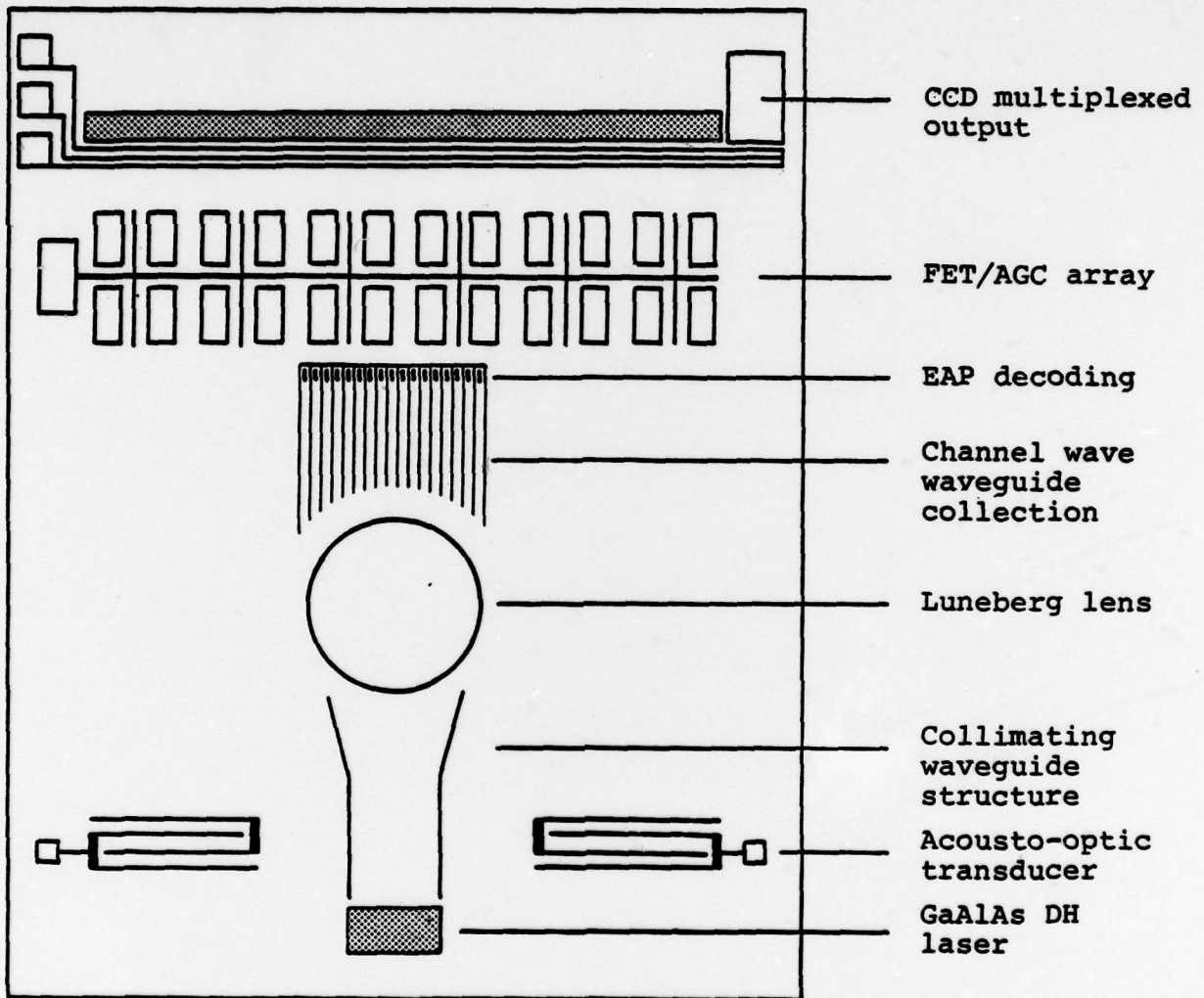
Figure 1. A hypothetical GaAs IOC for
real-time spectrum analysis.

in silicon. Further investigation and experimental development
are necessary, however, to assure optimum design and performance.

1.3   Waveguide Detector Array

One of the basic elements for a wide bandwidth spectrum ana-
lyzer is the waveguide detector array. Descrete GaAs avalanche
photodiodes[3] have been found to have a higher gain-bandwidth
product and an enhanced signal-to-noise ratio (30 dB), as compared
to silicon devices, because of the higher ratio of the hole-to-electron
ionization coefficients in GaAs[16]. In the electroabsorption ava-
lanche photodiode (EAP) mode of operation[8], these devices are
capable of detecting the below-bandgap GaAs laser emission with a
response time of less than 1 nsec[8]. Results for GaAs EAP devices
in waveguide configuration are equivalent to those for discrete
detectors[2]. Since both the gain and the absorption are bias-
controlled in the GaAs EAP devices, they have a dynamic range which
is orders-of-magnitude larger than silicon devices where only the
gain is bias controlled. For these reasons, we have developed an
array of GaAs EAP detectors in channel waveguides, where the bias
on each detector is controlled by an AGC circuit.

To determine the quality and dimensional constraints on the
detector array, we have to examine the operation of the spectrum
analyzer. The basic elements of the IOC spectrum analyzer consist
of a coherent source, an acousto-optical modulator which Bragg
diffracts the coherent light in proportion to the applied frequency

and amplitude, a lens which collects the diffracted light and Fourier transforms it into a spatial distribution, and the detector array which converts the spatially distributed optical radiation into electrical signals. Such a system based on waveguiding oxide layers on silicon substrates, has previously been analyzed[1].

From this analysis, the minimum resolvable frequency difference for a GaAs waveguide-based spectrum analyzer with an optical aperture of 1 cm would be 0.5 MHz. Assuming a GaAs laser wavelength of 0.91 μm and a Fourier transform lens focal length of 4 cm, a center-to-center photodiode spacing of about 1 μm would be required to detect this frequency difference. If the bandwidth of the input electrical signal were 200 MHz, an array of 400 elements spaced at 1 μm would be required. At the present time, the limits of photo-lithography make the fabrication of such an array impractical. A more practical scheme would be a 20 element array of GaAs EAP photo-diodes with a center-to-center spacing of 20 μm. For a Fourier transform lens focal length of 4 cm, which could be obtained by folding the optical axis on the waveguide, this spacing would give a minimum resolvable frequency difference of somewhat less than 10 MHz. For each detector in the array, a GaAs FET could be incorporated on the same chip to provide for automatic control of the bias which, in turn, would control both the gain and the absorption.

2. Fabrication

A design was chosen for the photodiode array in which the EAP detectors are contained in a channel waveguide structure. Each

channel is 20 μm wide and separated from adjacent channels by 20 μm as shown in Figure 2. The detectors are aluminum Schottky barriers 20 μm wide and 100 μm long on epitaxial GaAs ($N_D = 10^{15}$ cm^{-3}). The FET structure is shown in Figure 3. The source and drain contacts are each 200 by 120 μm. A 5 μm, aluminum, self-aligned gate is used with a source-to-drain spacing of 10 μm. A mesa structure is employed to provide isolation between channels, and thereby, mini- mize crosstalk. Five FET gates are connected to a common bonding pad to minimize connections.

Epitaxial material was produced by a two growth scheme. First, an n$^+$ layer is grown on half of the substrate followed by an n-type epitaxial layer over the whole substrate. The first layer provides the contact to the back of the photodiodes. The second layer serves as the active region for the diodes and the FETs. Samples were pro- cessed by standard lithographic techniques to achieve monolithic photodiodes and FETs. Unfortunately, the samples cleaved, separating the EAPs and the FETs. Further processing was then done independently. With the exception of this problem, all processing was quite success- ful and several working samples were obtained.

3. Evaluation

After processing, samples were cleaved and mounted on headers. Although different methods were tried, uniform cleaves were diffi- cult to achieve. This becomes a problem when trying to couple the laser to the waveguide. It is not possible to compensate for the quality of the cleave. Two lasers were used to achieve the entire
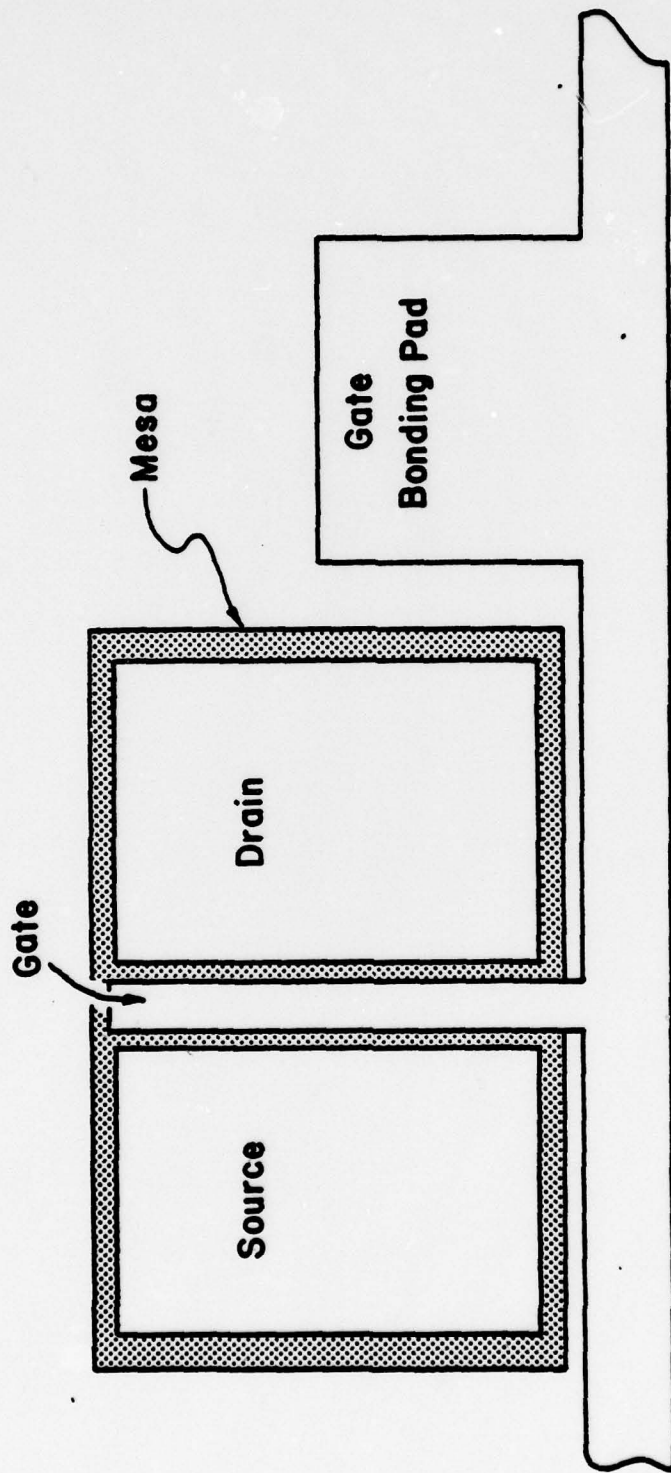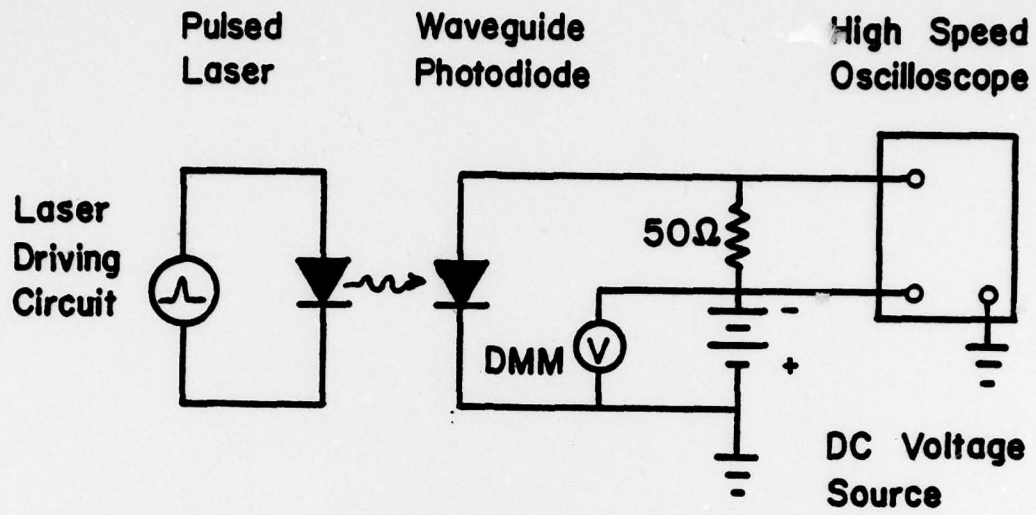
Figure 2. The channel waveguide structure with EAP detectors.

Figure 3.   The GaAs FET structure

dynamic range of the evaluation. For larger power levels, a 5 watt pulsed laser was used operating at 0.905 µm. Below 1 µwatt, a CW laser was used operating at 0.89 µm, and 5 milliwatt output. Although every attempt was made to obtain the data accurately, noise limited the dynamic range for both lasers. For pulsed operation, noise originated in the circuits used to drive the laser and was not due to the photodiode array. CW measurements were limited to variations in the dark current due to microplasma breakdowns. Although such breakdowns are fairly common, their effect can be minimized by careful material preparation and selection.

3.1   Equipment

A specially designed probing apparatus allowed easy mounting of the device headers. The device was viewed with a microscope allowing careful alignment of two tungsten probes. Movement of the probing apparatus was provided by an X-Y-Z-θ translator to place the device in the laser beam focal plane. The laser and associated optics were each mounted on X-Z translators fixed to a common X-Y translator. This common translator provided convenient scanning of the detector array. The optics chosen for focusing the laser beam were two infrared lenses and one microscope objective.

The electrical connections are shown in Figures 4 and 5. For pulsed operation, an oscilloscope was necessary to measure the response across the 50 ohm load. Two configurations are shown utilizing the scope single input and differential inputs. A slight

Pulsed
Laser

Waveguide
Photodiode

High Speed
Oscilloscope

Laser
Driving
Circuit

50Ω

DMM Ⓥ

−

+

DC Voltage
Source

(a)   Differential input to the scope

Pulsed
Laser

Waveguide
Photodiode

DC Voltage
Source

High Speed
Oscilloscope

Laser
Driving
Circuit

DMM Ⓥ

−

+

50Ω
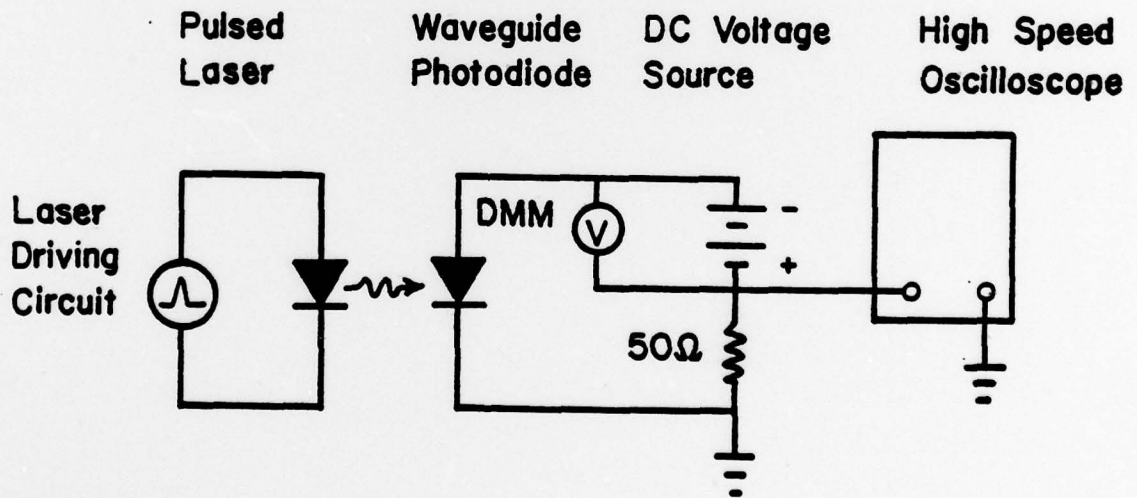
(b)   Single input to the scope

Figure 4.   Electrical connections
for pulsed measurements

CW Laser   Waveguide Photodiode

DC Current Source
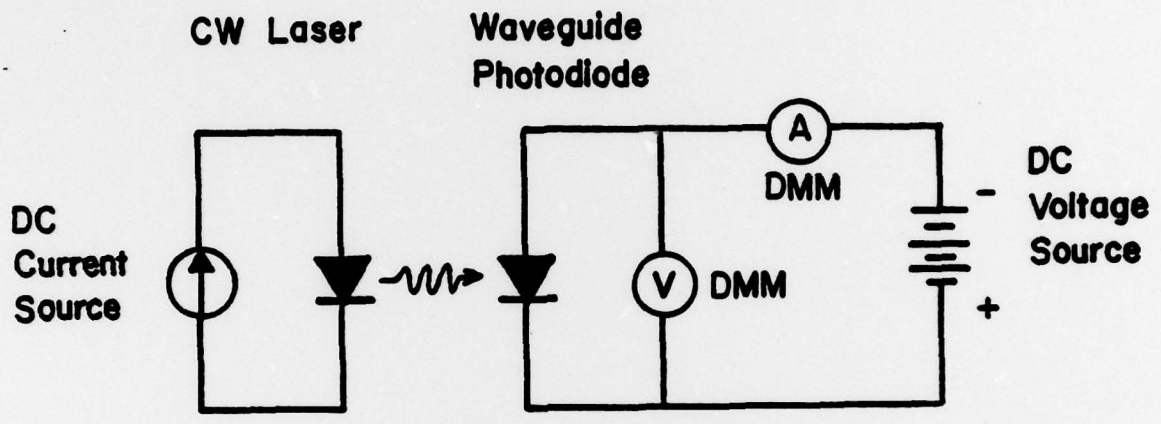
DMM (A)

DMM (V)

DC Voltage Source

Figure 5. Electrical connections
for CW measurements

reduction in noise was noticed for the differential mode, but some versatility and accuracy was also lost. All connections were made with standard 50 ohm coaxial cable and fittings to minimize noise pickup. For the CW measurements, the scope was not used, and the photocurrent was measured directly with a digital current meter. Coaxial cable was also used for these measurements to reduce noise.

3.2 Procedure

The pulsed laser was connected and set to operate at a 200 nsec pulse width and 2kHz PRF. This mode of operation results in a small duty cycle to maximize laser stability. A power meter was mounted in place of the detector during alignment. The optics were then arranged for maximum response. An aperture was placed at the beam focal point. The aperture size was 5 by 20 μm: the same as the waveguide input face. By measuring the power transmitted through this aperture, the amount of light incident on the waveguide could be calibrated. After calibration, the power meter and aperture were replaced by the waveguide photodetector array. The alignment was repeated for maximum response. Bias supplied to the detector was also varied for a maximum signal. Response at reduced power levels was then obtained by reducing the laser current and by introducing neutral density filters into the beam.

3.3 Results

Data have been collected using several detectors and a variety of techniques to insure the consistency of the results. Both pulsed

and CW lasers were necessary to achieve the high and low power levels, respectively. The accuracy of the data is limited to the values shown in Figure 6. This is a best case analysis and does not include errors due to locating a maximum in response or variations arising from the quality of the cleave.

3.3.1   Pulsed Laser Data

A row of 50 detectors was chosen for study. The first 30 of these were good quality, but the remaining 20 decreased in quality as the sample edge was approached. Each of the 30 was illuminated with the 0.905 µm laser at maximum power and at reduced power levels until the response was undetectable. All detectors were biased at the same dark current. The laser was swept along the array and maximized for each detector so as to reproduce the same illumination for each detector. These results are listed in Table 1. Next, a suitable detector was chosen for dynamic range data. For this detector the power was varied in smaller increments to provide a larger number of data points.

3.3.2   CW Laser Data

CW measurements were done only for the purpose of extending the dynamic range data. Power levels were set by using neutral density filters. The power was reduced until the response was no longer detectable. These data were obtained with a different detector than that obtained with the pulsed laser.
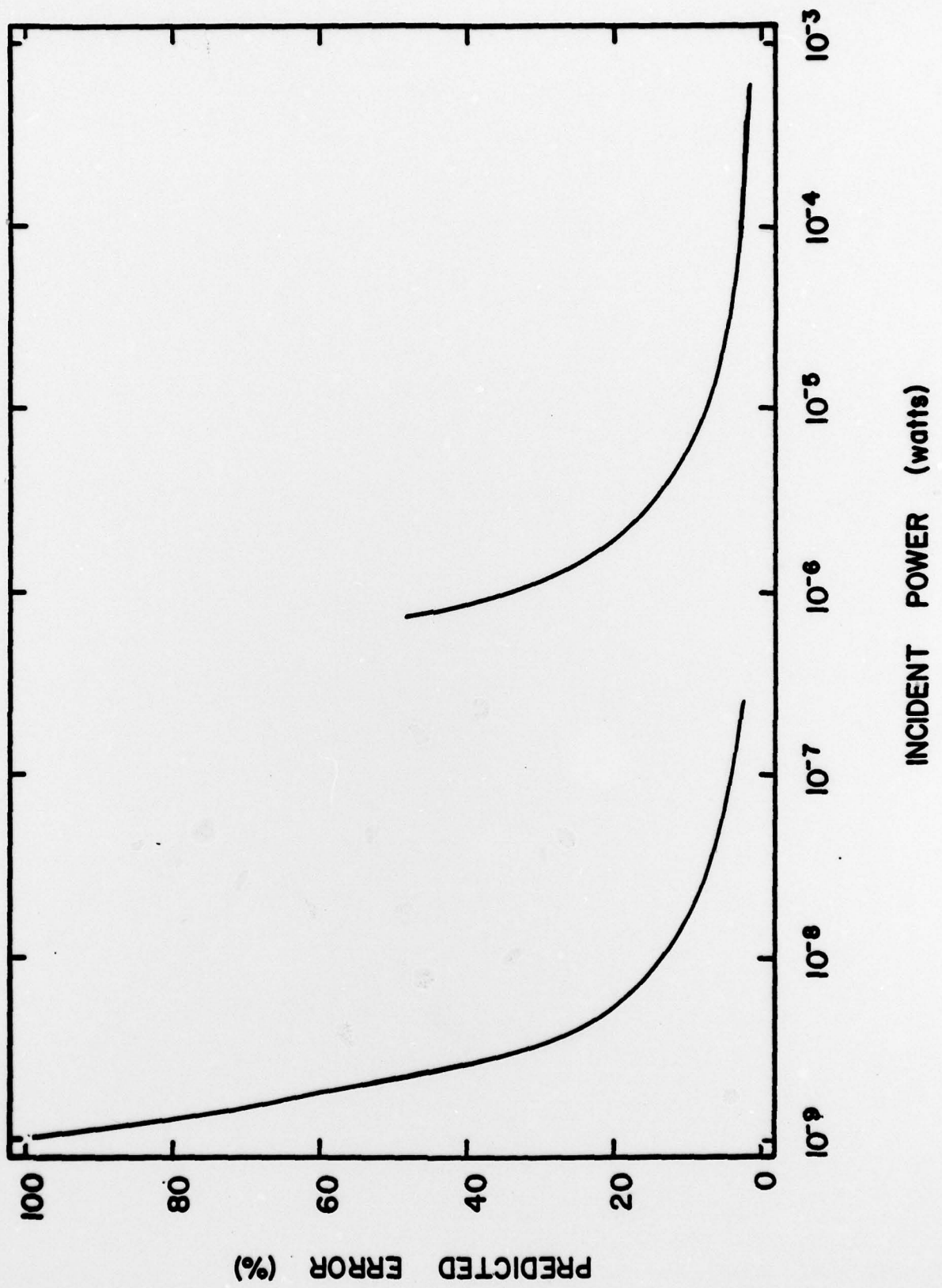
Figure 6. Predicted minimum error

Table 1
Response of Scanned 30 Element Array

element no.	Power level (dB)				bias voltage
	0	-4.3	-8.9	-13.2	
1	2.28	1.2	0.60	0.40	76
2	2.40	1.3	0.80	0.50	77
3	2.40	1.4	0.60	0.40	79
4	2.40	1.3	0.60	0.40	82
5	2.40	1.2	0.60	0.50	82
6	2.60	1.2	0.60	0.40	88
7	2.60	1.3	0.60	0.30	85
8	3.00	1.2	0.60	0.40	86
9	3.00	1.6	1.1	0.70	80
10	3.00	1.4	0.60	0.40	93
11	2.70	1.1	0.50	0.40	89
12	3.00	1.4	0.80	0.50	93
13	2.60	1.3	0.60	0.20	87
14	3.20	1.8	0.60	0.20	90
15	2.90	1.5	0.70	0.40	93
16	3.20	1.6	0.60	0.30	94
17	2.80	1.4	0.50	0.30	93
18	2.80	1.0	0.30	----	86
19	2.00	0.6	0.10	----	90
20	3.80	1.8	1.00	0.30	94
21	3.20	1.6	0.50	0.40	95
22	4.50	2.2	1.2	0.60	96
23	4.60	2.2	0.90	0.50	102
24	3.60	2.4	1.4	0.60	104
25	3.20	1.4	0.80	0.60	102
26	4.00	1.6	1.2	0.80	103
27	4.20	2.8	1.2	0.40	97
28	2.40	1.6	0.20	0.40	100
29	2.30	1.2	0.60	0.30	95
30	2.00	1.2	0.40	0.20	110

4.   Analysis

The role of the waveguide photodiode array is crucial in pro-
viding accurate Fourier transform data in a spectrum analyzer. Any
analysis of the array must take into account the dynamic range re-
quirements as well as the uniformity of the response. Crosstalk
must be minimized to allow the full use of the dynamic range.

4.1   Dynamic Range

Photoresponse has been measured for a total power range of
57 dB. The data taken with the pulsed laser account for 29 dB
and the remaining 28 dB were taken with the CW laser. A curve was
fitted to this data by linear regression. Deviations from the curve
were then computed both in percent and in dB. Table 2 lists the
data along with the computed deviations from the curve. The data
are plotted along with the curve in Figure 7. Figures 8 and 9 are
plots of the deviations. The equation for the best fit curve is as
follows:

$$I_{ph} = k \ (P)^{0.5182}$$

where I_{ph} is the photoresponse

P   is the incident power

$k = 0.1012$; I_{ph} (amps), P (watts)

or   78.67 ; I_{ph} (μamps), P (μwatts)

Deviations must be considered with respect to the error estimate
given in Figure 6.

Table 2

Dynamic range data

| P_i(uwatt)	I_p(uamp)	$I_p"$(uamp)	$\dfrac{I_p - I_p"}{I_p}$ (%)	$10 \log (I_p/I_p")$
540	2600	2051	26.8	1.03 dB
188	1150	1187	- 3.1	-0.14
75	640	737	-13.2	-0.61
70	620	711	-12.8	-0.59
64	600	679	-11.6	-0.54
53	580	616	- 5.8	-0.26
44	520	559	- 7.0	-0.31
35	500	497	0.6	0.03
26	460	426	8.0	0.33
22	400	390	2.6	0.11
14	320	309	3.6	0.15
9.0	260	246	5.7	0.24
6.0	200	199	0.5	0.02
3.5	160	151	6.0	0.25
2.2	120	118	1.7	0.07
0.7	40	65.4	-39	-2.1
0.23	39	36.7	6.3	0.26
0.068	21	19.5	7.7	0.32
0.025	12	11.6	3.4	0.15
0.0075	6	6.23	-3.7	-0.16
0.0037	4	4.32	-8.0	-0.33
0.0011	1	2.31	-53	-3.6
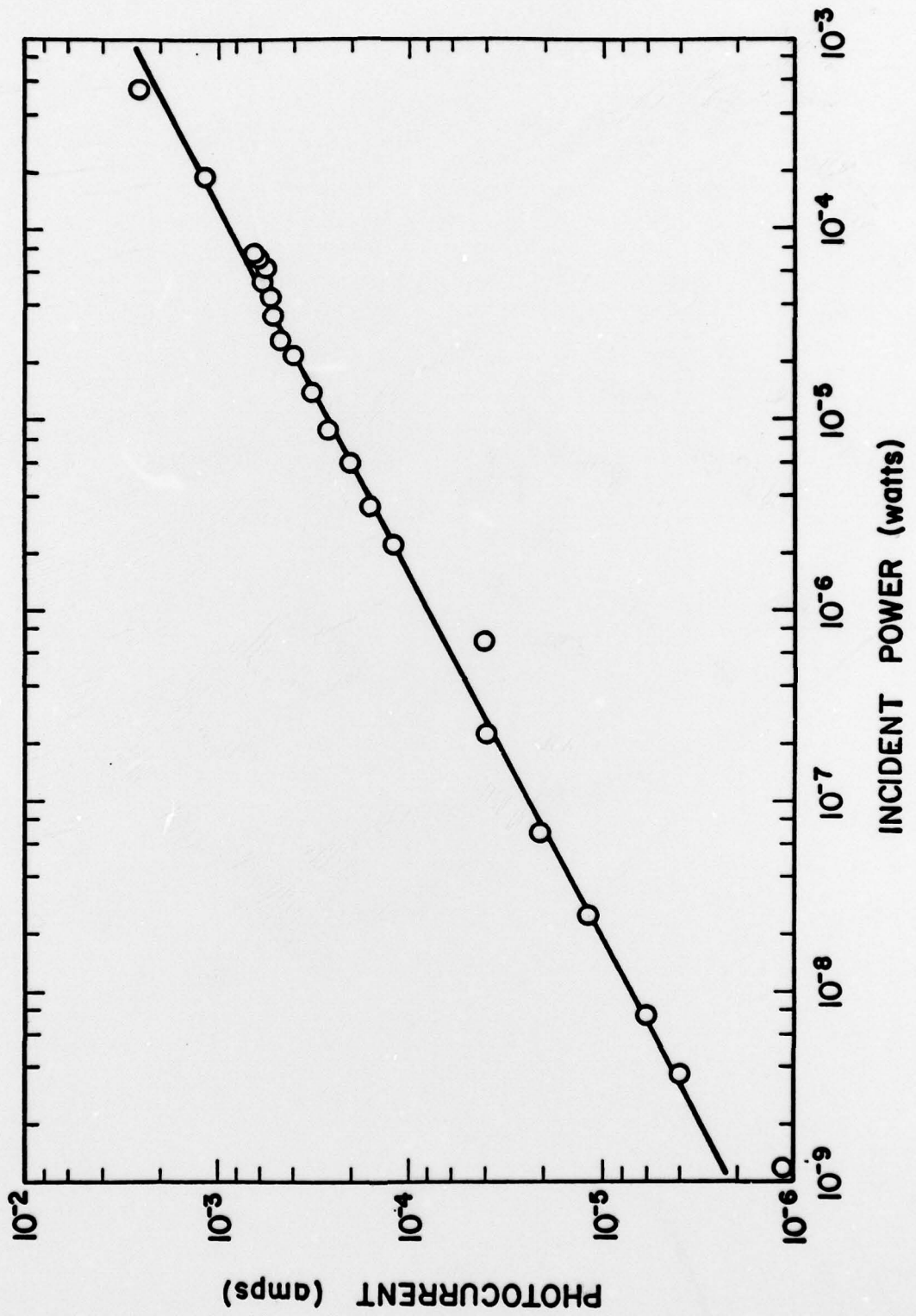
Figure 7. Response characteristic
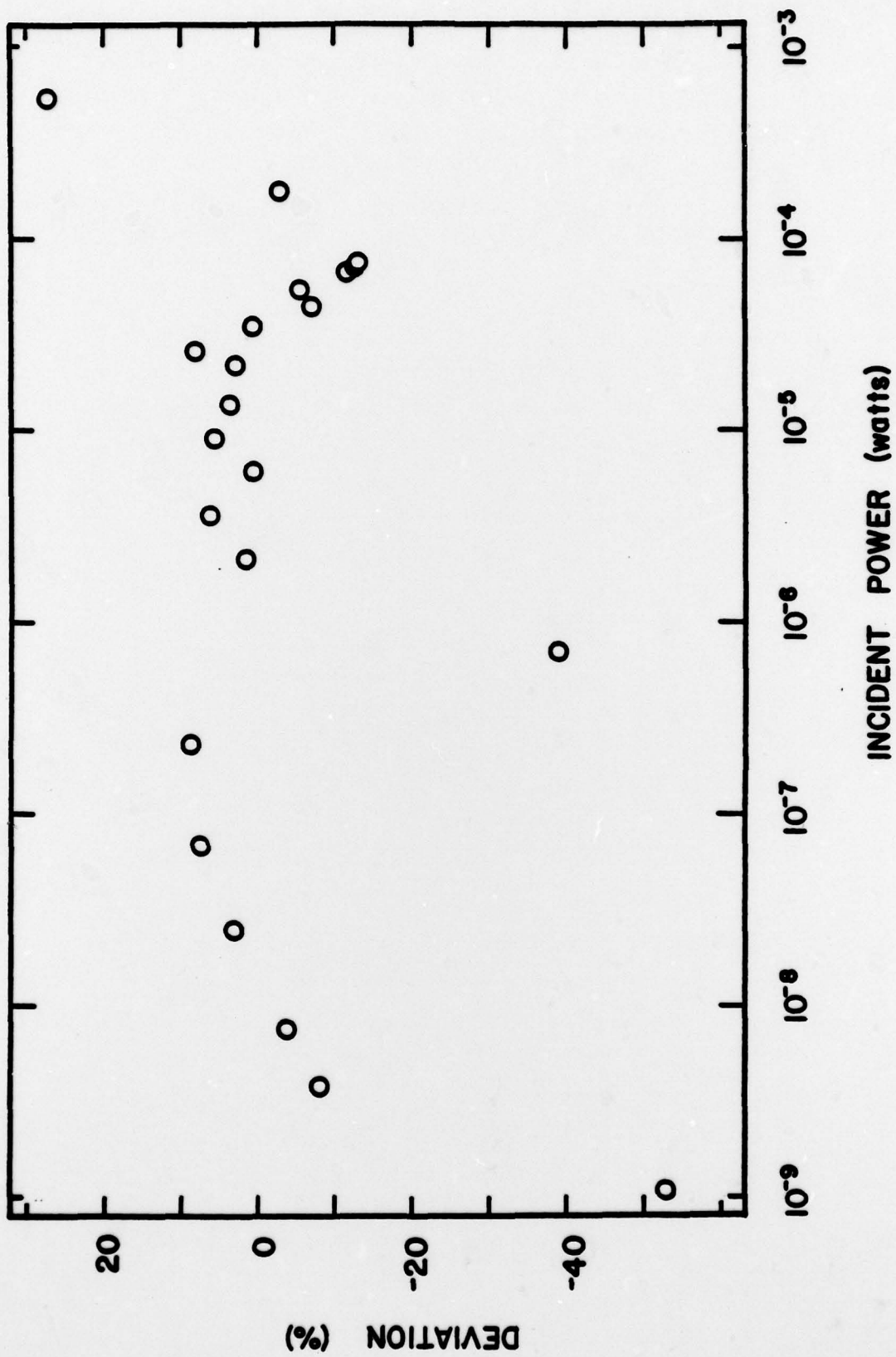
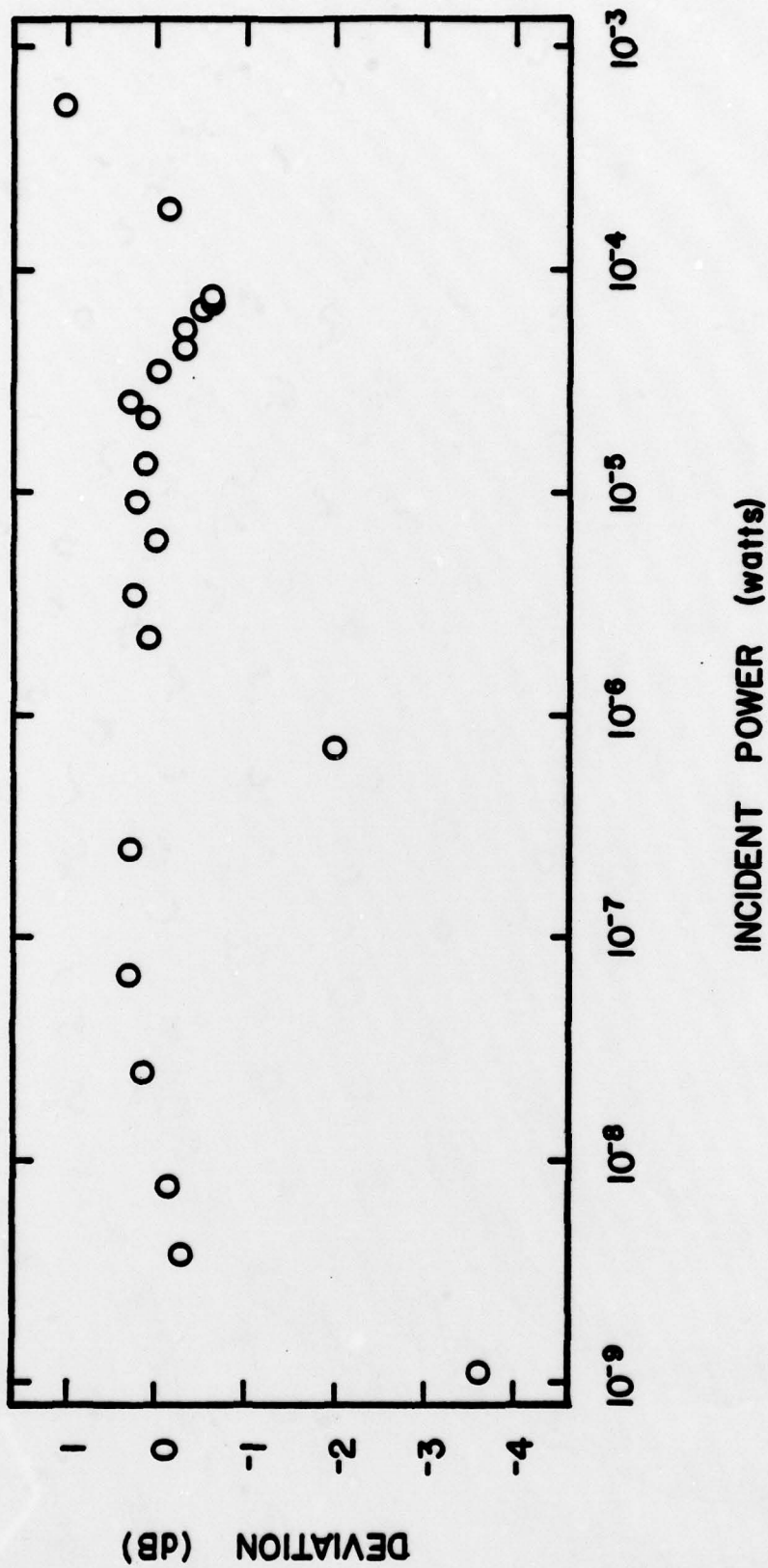Figure 8. Deviation of response from
best fit curve

Figure 9. Deviation of response from
best fit curve

4.2 Channel-to-channel Tracking

The analysis of 30 adjacent photodiodes provided information on response uniformity. Each detector was illuminated in the same way and at the same power levels. Therefore, any variation is due to the variation in the photodiode. The response data (as given in Table 1) are summarized in Table 3. Variations here may be largely due to the varying quality of the cleave and the difficulty of using the neutral density filters.

4.3 Crosstalk

This parameter was very difficult to measure as it required optical isolation of one waveguide from an adjacent one. Once this condition was achieved, the measurement was still limited to about 30 dB due to the instrument sensitivity. Measurements at maximum power illumination did not reveal any response in the adjacent detectors due to crosstalk so it can be assumed to be better than 30 dB.

5. Conclusions

The results of this evaluation are very promising. The waveguide photodiodes have shown a dynamic range of nearly 60 dB and possibly greater. This range is compatible with present CW laser emission levels for optimum coupling. The response characteristic is not logarithmic, but represents a good deal of compression compared to a linear response. Device uniformity is better than

Table 3

Tracking of Waveguide Detector Array

Detector Numbers	Laser Power Attenuation (dB)	Photoresponse Mean, M (ma)	Standard Deviation, δ (ma)	$10 \log \frac{(M+\delta)}{M}$ (dB)
1 to 30	0	3.16	0.736	0.91
1 to 20	0	2.93	0.432	0.60
1 to 20	- 4.3	1.41	0.289	0.81
1 to 20	- 8.9	0.660	0.226	1.3
1 to 20	-13.2	0.414	0.126	1.2

15% (0.60 dB) for 20 devices. This is one area that can certainly be improved, since these were not exceptional devices. The measured crosstalk is quite reasonable, but should be exam ed more closely to be complete. The results of these measurements and analysis are summarized in Table 4.

Table 4
Summary of Evaluation

Power Range: 1.1 uwatt to 0.540 watt

Response Range: 1 namp to 2.6 mamp

Dynamic Range: 57 dB

Response Linearity: $\pm$ 7%, ($\pm$ 0.3 dB)   from mean

maximum, +26% (1.0 dB)

· -13% (0.6 dB)

Crosstalk: better than 30 dB between adjacent channels

Channel-to-channel Tracking:

30 adjacent detectors, 23% (0.91 dB)

20 adjacent detectors   15% (0.60 dB)

6.   References

(1)   Anderson, D. B., J. T. Boyd, M. C. Hamilton, and R. R. August, *IEEE Journal of Quantum Electronics*, to be published.

(2)   Sun, M. J., K. H. Nichols, W. S. C. Chang, R. O. Gregory, F. J. Rosenbaum, and C. M. Wolfe, *Applied Optics*, 17, 1568, 1978.

(3)   Lindley, W. T., R. J. Phelan Jr., C. M. Wolfe, and A. G. Foyt, Applied Physics Letters, 14, 197, 1969.

(4)   Stillman, G. E., C. M. Wolfe, J. A. Rossi, H. Heckscher, *Applied Physics Letters*, 28, 197, 1976.

(5)   Hurwitz, C. E., J. A. Rossi, J. J. Hseih, and C. M. Wolfe, *Applied Physics Letters*, 27, 241, 1975.

(6)   Franz, W., "Einflu eines elektrischen Feldes auf eine optische Absorptionskante", *Zeitschrift Naturforsch*, A 13, 494, 1958.

(7)   Keldysh, L. V., *Journal of Experimental and Theoretical Physics (USSR)*, 34, 1138, 1958.

(8)   Stillman, G. E., C. M. Wolfe, J. A. Rossi, and J. L. Ryan, *Institute of Physics Conference Series*, 24, Chapter 4, 1975.

(9)   Anderson, D. B., R. R. August, J. E. Coker, *Applied Optics*, 13, 2742, 1974.

(10)   Wang, S., *IEEE Journal of Quantum Electronics*, QE-10, 413, 1974.

(11)   Kuhn, L., M. L. Dakss, P. F. Heidrich, and B. A. Scott, *Applied Physics Letters*, 17, 265, 1970.

(12)   Loh, K. W., W. S. C. Chang, W. R. Smith, and T. Grudkowski, *Applied Optics*, 15, 156, 1976.

(13)   GiaRusso, D. P., and J. H. Harris, Applied Optics, 10, 2786, 1971.

(14) Shubert, R., and J. H. Harris, <u>Journal</u> <u>of</u> <u>the</u> <u>Optical</u>
      <u>Society</u> <u>of</u> <u>America</u>, 61, 154, 1971.

(15) Deyhimey, K., J. H. Harris, D. D. Ewall, and R. C. Eden,
      paper presented at 36th Device Research Conference, University of California, Santa Barbara, June 1978.

(16) Stillman, G. E., C. M. Wolfe, J. A. Rossi, and A. G. Foyt,
      <u>Applied</u> <u>Physics</u> <u>Letters</u>, 24, 471, 1974.